Bioorganic Chemistry 83 (2019) 559–568

Contents lists available at ScienceDirect

Bioorganic Chemistry

journal homepage: www.elsevier.com/locate/bioorg

Synthesis and biological evaluation of new *N*-benzylpyridinium-based benzoheterocycles as potential anti-Alzheimer's agents

Naeimeh Salehi[a], Bi Bi Fatemeh Mirjalili[a,*], Hamid Nadri[b], Zahra Abdolahi[b], Hamid Forootanfar[c], Alireza Samzadeh-Kermani[d], Tuba Tüylü Küçükkılınç[e], Beyza Ayazgok[e], Saeed Emami[f], Ismaeil Haririan[g], Mohammad Sharifzadeh[h], Alireza Foroumadi[i,j], Mehdi Khoobi[k,l,*]

[a] Department of Chemistry, College of Science, Yazd University, Yazd, P.O. Box 89195-741, Iran
[b] Faculty of Pharmacy, Shahid Sadoughi University of Medical Sciences, Yazd, Iran
[c] Department of Pharmaceutical Biotechnology, Faculty of Pharmacy, Kerman University of Medical Sciences, Kerman, Iran
[d] Department of Chemistry, Faculty of Sciences, University of Zabol, Zabol, Iran
[e] Hacettepe University, Faculty of Pharmacy, Department of Biochemistry, Ankara, Turkey
[f] Department of Medicinal Chemistry and Pharmaceutical Sciences Research Center, Faculty of Pharmacy, Mazandaran University of Medical Sciences, Sari, Iran
[g] Department of Pharmaceutical Biomaterials, Medical Biomaterials Research Center, Faculty of Pharmacy, Tehran University of Medical Sciences, Tehran, Iran
[h] Department of Pharmacology and Toxicology, Faculty of Pharmacy, Toxicology and Poisoning Research Centre, Tehran University of Medical Sciences, Tehran, Iran
[i] Neuroscience Research Center, Institute of Neuropharmacology, Kerman University of Medical Sciences, Kerman, Iran
[j] Department of Medicinal Chemistry, Faculty of Pharmacy, Tehran University of Medical Sciences, Tehran, Iran
[k] The Institute of Pharmaceutical Sciences (TIPS), Tehran University of Medical Sciences, Tehran 1417614411, Iran
[l] Departmnt of Pharmaceutical Biomaterials, Medical Biomaterials Research Center, Faculty of Pharmacy, Tehran University of Medical Sciences, Tehran, Iran

ARTICLE INFO

Keywords:
Alzheimer's disease
Benzothiazole
Pyridinium
AChE
Aβ aggregation
Neuroprotection

ABSTRACT

A novel series of benzylpyridinium-based benzoheterocycles (benzimidazole, benzoxazole or benzothiazole) were designed as potent acetylcholinesterase (AChE) and butyrylcholinesterase (BuChE) inhibitors. The title compounds **4a-q** were conveniently synthesized *via* condensation reaction of 1,2-phenylenediamine, 2-aminophenol or 2-aminothiophenol with pyridin-4-carbalehyde, followed by *N*-benzylation using various benzyl halides. The results of in vitro biological assays revealed that most of them, especially **4c** and **4g**, had potent anticholinesterase activity comparable or more potent than reference drug, donepezil. The kinetic study demonstrated that the representative compound **4c** inhibits AChE in competitive manner. According to the ligand-enzyme docking simulation, compound **4c** occupied the active site at the vicinity of catalytic triad. The compounds **4c** and **4g** were found to be inhibitors of Aβ self-aggregation as well as AChE-induced Aβ aggregation. Meanwhile, these compounds could significantly protect PC12 cells against H_2O_2-induced injury and showed no toxicity against HepG2 cells. As multi-targeted structures, compounds **4c** and **4g** could be considered as promising candidate for further lead developments to treat Alzheimer's disease.

1. Introduction

Memory problems in elderly people could be symptoms of Alzheimer's disease (AD), an irreversible neurodegenerative brain disease causing progressive deterioration of memory, thinking and reasoning skills. AD is currently one of the top leading causes of death among older adults. It is estimated that the number of AD patients rises by more than 11 million people per year, which leads to a tremendous burden on the society and the family [1].

AD is a complex multifactor disease that its exact pathogenesis is not fully clear. Neuropathological studies have demonstrated that the low levels of acetylcholine, β-amyloid plaques formation within the brain of AD patients and oxidative damage of neuronal cells are the key factors for the development of AD [2]. Deficiency of acetylcholine is caused by the disturbed activity of two types of cholinesterase enzymes, namely acetylcholinesterase (AChE) and butyrylcholinesterase (BuChE), which hydrolyze acetylcholine into the inactive metabolites, choline and acetate [3]. Cholinesterase inhibitors are employed to reduce acetylcholine (ACh) breakdown, thereby increasing the concentration of acetylcholine neurotransmitter in the brain. Structural studies on AChE showed that this enzyme has two binding site, catalytic anionic site (CAS) and peripheral anionic site (PAS). It was proved that dual binding

* Corresponding authors at: The Institute of Pharmaceutical Sciences (TIPS), Tehran University of Medical Sciences, Tehran 1417614411, Iran (M. Khoobi).
E-mail addresses: fmirjalili@yazd.ac.ir (B.B.F. Mirjalili), m-khoobi@tums.ac.ir (M. Khoobi).

https://doi.org/10.1016/j.bioorg.2018.11.010
Received 23 June 2018; Received in revised form 25 August 2018; Accepted 10 November 2018
Available online 13 November 2018
0045-2068/

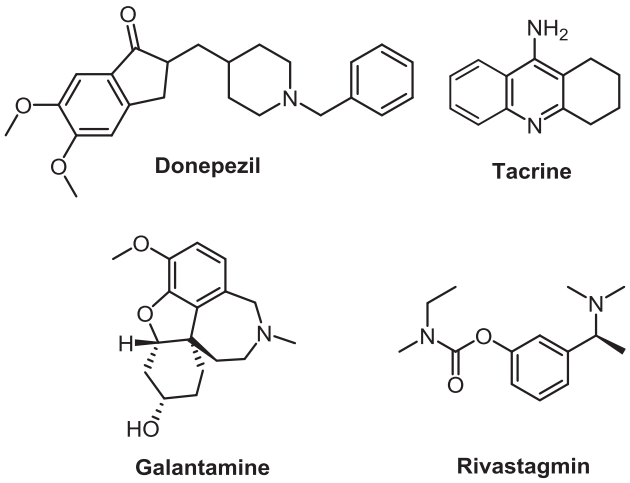

Fig. 1. Chemical structures of known AChE inhibitors.

site (DBS) AChE inhibitors were more potent inhibitors compared to the compounds that interact with only one site of the enzyme [4,5]. The most prescribed cholinesterase inhibitors such as donepezil, tacrine, rivastigmine, and galantamine (Fig. 1) can improve neuropsychiatric symptoms such as agitation or depression but are not able to delay or halt the progression of the disease [6].

Several studies have provided evidences that amyloid β (Aβ) and its precursor protein (APP) have physiological role in the brain. However, progressive accumulation of Aβ protein is an important factor in the development of AD. Abnormal accumulation of Aβ is the result of an imbalance between Aβ production, aggregation and clearance [7]. Furthermore, the peripheral anionic site of AChE plays a key role in accelerating Aβ plaques deposition [8]. On the other hand, transformation of an initial benign form of senile plaque to a malignant form associated with AD is facilitated by BuChE [9]. In initial stages of the neurodegenerative process, Aβ could enter the mitochondria and increase the production of reactive oxygen species (ROS) by disrupting the electron transport chain and induce oxidative stress [10]. Therefore, prevention of Aβ aggregation and formation of free radicals or protecting the cells against oxidative stress by neuroprotective agents will be a promising strategy for AD pharmacotherapy.

Molecular modeling and crystal structure of AChE complex with donepezil have shown that the benzylpiperidine group of donepezil interacts with the indole ring of Trp84 of anionic subsite and the indanone ring has a parallel π-π interaction with indole ring of Trp279 at the peripheral site of AChE enzyme [11]. The pharmacological profile of donepezil has attracted the attention of researchers on design and synthesis of donepezil-like compounds as potential anti-Alzheimer's agents. Many new cholinesterase inhibitors have been synthesized by replacement of indanone ring in donepezil with different aromatic and heteroaromatic systems [12–15]. Amine-derived groups such as phenylpiperazine, benzylpyridinium and benzylamine are also capable to interact with the catalytic site of the AChE, like benzylpiperidine moiety of donepezil [16–18]. Considering these scaffolds, our group has previously reported some potent AChE inhibitors such as **I** and **II**, in which the *N*-benzylpyridinium moiety as an essential part for superior activity was attached to a series of heteroaromatic scaffolds (Fig. 2) [19,20].

Benzothiazoles have assumed especial significance in pharmaceutical chemistry, as well as in drug discovery. Some benzothiazole derivatives strongly interact with Aβ peptides and can reduce the soluble amyloid oligomers burden [21–24]. In particular, the 2-arylbenzothiazole pharmacophore is known to have high affinity for Aβ. For example, 2-(4′-methylaminophenyl)benzothiazole (BTA-1, **III**) is an uncharged derivative of thioflavin-T that has high affinity for amyloid deposits and good blood brain barrier (BBB) permeability [21]. Also, Huang et al. have reported a series of tacrine–phenylbenzothiazole conjugates as multifunctional anti-Alzheimer's disease agents. Typically, compound **IV** was the most potent AChE inhibitor (IC_{50} = 0.017 μM) with Aβ aggregation inhibitory activity [22]. Thus, this type of molecules containing a 2-arylbenzothiazole pharmacophore can be used as suitable diagnostic imaging agents and potential therapies for Alzheimer's disease.

Due to the importance of multi-target drugs development for AD therapy and on the basis of the above-mentioned findings, we have designed a novel hybrid series of donepezil-like compounds bearing benzoheterocyclic and benzylpyridinium moieties (Fig. 2). The designed compounds were synthesized and evaluated for multifunctional biological activities including anti-cholinesterase, $Aβ_{1-42}$ protein anti-aggregating, and protective effect against H_2O_2-induced PC12 cell injury, as well as docking study.

2. Results and discussion

2.1. Chemistry

The designed compounds 4-(1*H*-benzo[*d*]imidazol-2-yl)-1-benzylpyridinium bromide (**4a**), 4-(benzo[*d*]oxazol-2-yl)-1-benzylpyridinium bromide (**4b**) and 4-(benzo[*d*]thiazol-2-yl)-1-benzylpyridinium halides **4c-q** were easily prepared in two steps (Scheme 1). In the first step, 2-(pyridin-4-yl)benzo[*d*]imidazole (**3a**), 2-(pyridin-4-yl)benzo[*d*]oxazole (**3b**) and 2-(pyridin-4-yl)benzo[*d*]thiazole (**3c**) were synthesized using different protocols.

Several catalysts were screened for the condensation of *o*-phenylenediamine (**1a**) and pyridin-4-carbalehyde (**2**) under various conditions (Table 1), but the best result was obtained using Fe_3O_4@nano-cellulose–OPO_3H (Fe_3O_4@NCs–OPO_3H) in EtOH at 50 °C. Reaction between 2-aminophenol (**1b**) and pyridin-4-carbalehyde (**2**) in the presence of $KMnO_4$/HOAc produced 2-(pyridin-4-yl)benzo[*d*]oxazole (**3b**) [25]. For preparation of 2-(pyridin-4-yl)benzo[*d*]thiazole (**3c**), 2-aminothiophenol (**1c**) and pyridin-4-carbalehyde (**2**) were condensed in the presence of Fe_3O_4@NCs–OPO_3H under various conditions, as listed in Table 1.

It was found that the best condition is under solvent-free condition at 100 °C. The simple isolation of products in pure form at excellent yields without the use of chromatography and affordable synthesis are important features of the applied protocols. At the final step, target products **4a-q** were obtained from the reaction of compounds **3a-c** with benzyl halides in dry acetonitrile under reflux conditions with excellent yields.

2.2. Inhibitory activity against AChE

The inhibitory activity of the synthesized compounds **4a-q** was assessed in vitro against AChE in comparison with commercially available drug donepezil as reference. The obtained IC_{50} values in nM were listed in Table 2. According to the screening data, benzothiazole derivatives **4c**, **4f**, **4g**, and **4h** have potent anti-AChE activity comparable or more potent than standard drug donepezil (IC_{50} values = 14–23 nM). Among them, 4-(benzothiazol-2-yl)-1-benzylpyridinium analogue **4c** with the IC_{50} value of 14 nM showed the highest activity against AChE. The comparison of unsubstituted compound **4c** with substituted benzyl analogues **4d-q** revealed that introduction of different substituents diminished the anti-AChE activity of the target compounds. The attenuation of the anti-AChE activity mainly depends on the position and electronic features of the substituents. In the *ortho*-substituted series, the hydrophobic substituent such as chlorine was more favorable than others. The movement of methyl group from *ortho*-position to *meta*-position led to positive effect on anticholinesterase activity (compare **4g** with **4d**). The anticholinesterase activity of *meta*-halobenzyl compounds showed that flouoro group is better than chloro and bromo substituents. In the *para*-substituted congeners, the compounds **4k** and

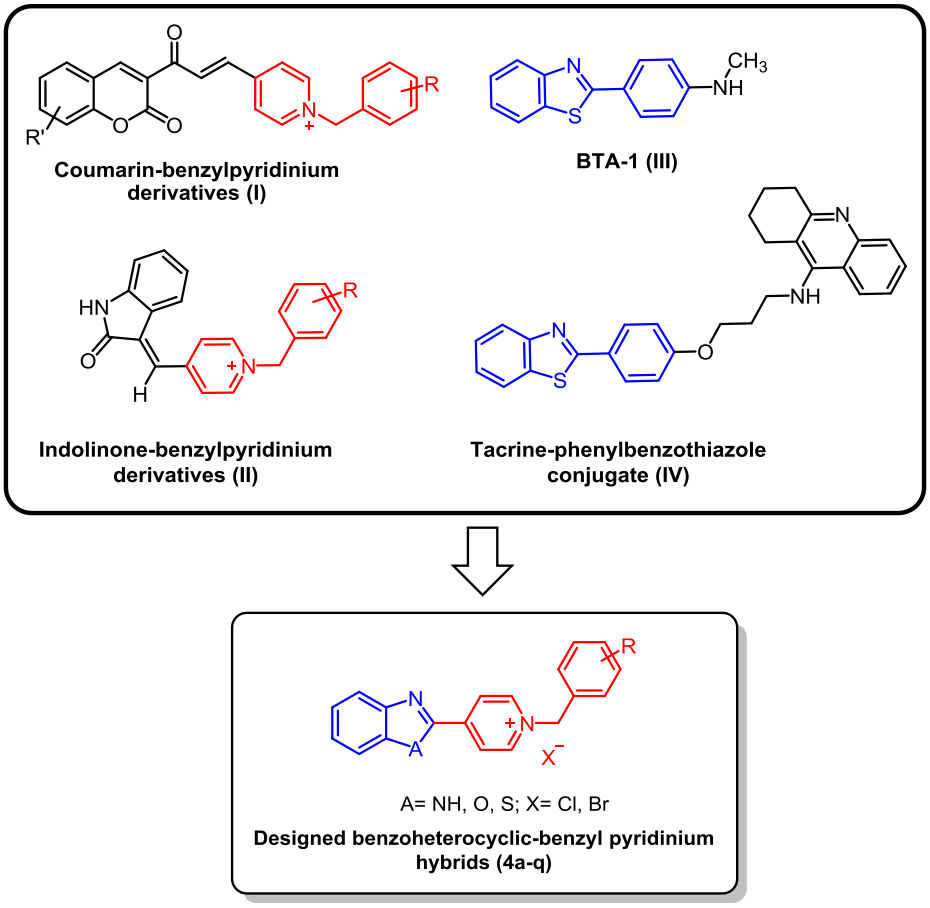

Fig. 2. Structures of previously reported compounds (**I-IV**) and newly designed compounds **4a-q**.

4m were less potent against AChE comparing to **4l**. The electron withdrawing nitro group more significantly decreased the activity as shown by compounds **4e** and **4k**, while the small electron withdrawing groups such as fluorine atom on phenyl ring led to good inhibitory potency against AChE (**4h** and **4l**). The introduction of second chlorine atom at *ortho* or *meta* positions (**4o** and **4p**) of 2-chlorobenzyl derivative **4f** resulted in a decrease in AChE inhibitory activity whereas the insertion of fluorine at *ortho* position (**4n**) presented the same activity.

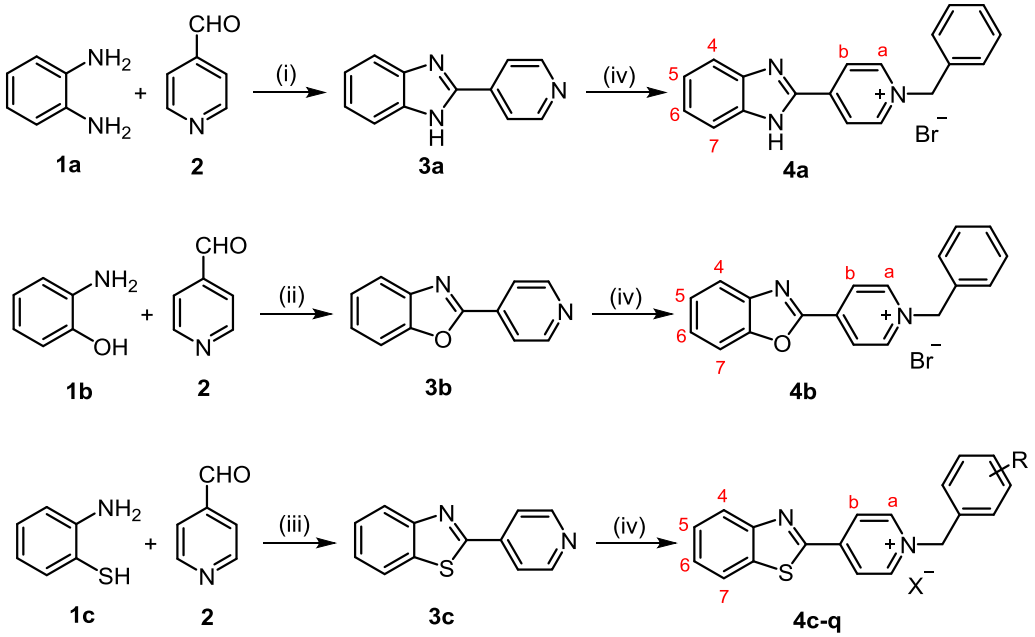

Scheme 1. Synthesis of target compounds **4a-q**. *Reagents and conditions*: (i) Fe_3O_4@nano-cellulose–OPO_3H, EtOH, 50 °C; (ii) $KMnO_4$/HOAc, r.t., grinding; (iii) Fe_3O_4@nano-cellulose–OPO_3H, solvent-free, 100 °C; (iv) appropriate benzyl halide, acetonitrile, reflux.

Table 1
The synthesis of 2-(pyridin-4-yl)-1*H*-benzo[*d*]imidazole (**3a**) and 2-(pyridin-4-yl)-benzo[*d*]thiazole (**3c**) under various conditions.[a]

Entry	Reactant	Catalyst (g)	Solvent	Conditions	Product	Time (h)	Yield[b] (%)
1	**1a**	$Al(HSO_4)_3$	EtOH	Reflux	**3a**	3	45
2	**1a**	Nano-$SnCl_4.SiO_2$ (0.05)	EtOH	Reflux	**3a**	3	72
3	**1a**	Nano-BF_3.Cellulose (0.05)	EtOH	Reflux	**3a**	3	65
4	**1a**	Nano-Silica sulfuric acid (0.05)	EtOH	Reflux	**3a**	3	77
5	**1a**	Fe_3O_4@NCs–OPO_3H (0.05)	EtOH	Reflux	**3a**	3	82
6	**1a**	Fe_3O_4@NCs–OPO_3H (0.05)	H_2O	Reflux	**3a**	3	10
7	**1a**	Fe_3O_4@NCs–OPO_3H (0.05)	S. F.[c]	70 °C	**3a**	3	25
8	**1a**	Fe_3O_4@NCs–OPO_3H (0.05)	EtOH	50 °C	**3a**	2	92
9	**1a**	Fe_3O_4@NCs–OPO_3H (0.05)	EtOH	r. t.	**3a**	2	68
10	**1c**	Fe_3O_4@NCs–OPO_3H (0.05)	EtOH	Reflux	**3c**	2	75
11	**1c**	Fe_3O_4@NCs–OPO_3H (0.05)	H_2O	Reflux	**3c**	2	15
12	**1c**	Fe_3O_4@NCs–OPO_3H (0.05)	EtOH	50 °C	**3c**	2	68
13	**1c**	Fe_3O_4@NCs–OPO_3H (0.05)	S. F.	120 °C	**3c**	1.5	88
14	**1c**	Fe_3O_4@NCs–OPO_3H (0.05)	S. F.	100 °C	**3c**	1.5	94
15	**1c**	Fe_3O_4@NCs–OPO_3H (0.05)	S. F.	80 °C	**3c**	1.5	80

[a] The ratio of compounds **1a** or **1c** (mmol) and **2** (mmol) is equal to 1:1.
[b] Isolated yield.
[c] Solvent free.

Table 2
Inhibitory activity of the target compounds **4a-q** against AChE and BuChE.

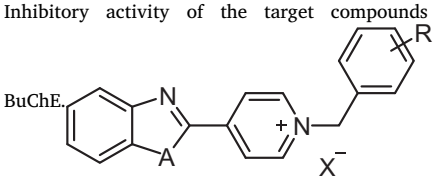

Compound	A	R	X	AChE IC_{50} (nM)	BuChE IC_{50} (nM)
4a	NH	H	Br	147 ± 8.3	930 ± 10.4
4b	O	H	Br	100 ± 4.2	280 ± 9.8
4c	S	H	Br	14 ± 0.7	182 ± 5.6
4d	S	2-CH_3	Cl	30 ± 2.9	2200 ± 68
4e	S	2-NO_2	Cl	159 ± 14.6	331 ± 11.2
4f	S	2-Cl	Cl	22 ± 1.5	348 ± 6.3
4g	S	3-CH_3	Cl	21 ± 1.8	523 ± 13.4
4h	S	3-F	Cl	23 ± 0.6	720 ± 13.6
4i	S	3-Cl	Br	61 ± 3.2	536 ± 7.7
4j	S	3-Br	Br	53 ± 1.3	800 ± 12.4
4k	S	4-NO_2	Cl	1900 ± 36	2100 ± 33
4l	S	4-F	Cl	36 ± 0.8	646 ± 4.6
4m	S	4-Br	Cl	> 300	> 3000
4n	S	2-Cl,6-F	Cl	27 ± 1.4	400 ± 1.8
4o	S	2,6-Cl_2	Cl	78 ± 5.7	379 ± 8.9
4p	S	2,4-Cl_2	Cl	> 300	748 ± 11.6
4q	S	3,4-Cl_2	Cl	> 300	> 3000
Donepezil	–	–		23 ± 1.3	3400 ± 23

[a]Data are expressed as mean ± S.E. of at least three different experiments.

Notably, the comparison of compound **4c** with its analogues **4a** or **4b** revealed that replacement of S by O or NH had no favorable effect on anti-AChE activity.

2.3. BuChE inhibitory activity

Given the increasing of BuChE activity in advanced AD patients, its inhibition as a treatment strategy may be valuable in the management of AD [26]. Consequently, in vitro effect of target compounds against BuChE was also assayed by the same method. As depicted in Table 2, the anti-BuChE activity of some tested compounds was superior to standard drug donepezil (IC_{50} values = 182–2200 nM). In particular, compound **4c** with IC_{50} value of 182 nM was 18-fold more potent than donepezil. Generally, the anti-BuChE activity of substituted benzyl analogs was less than unsubstituted counterpart **4c**. Nevertheless, the 2-nitro, 2-chloro, 2-chloro-6-fluoro and 2,6-dichloro derivatives (**4e**, **4f**, **4n**, and **4o** respectively) with IC_{50} values ≤ 400 nM were at least 8 times more potent than donepezil against BuChE. Based on the results gathered in the Table 2, the inhibitory activity of all compounds against AChE was higher over BuChE.

2.4. Inhibition of AChE-induced and self-induced Aβ aggregation

The amyloid-beta protein ($A\beta_{1\text{-}42}$) anti-aggregating activity of compounds **4c** and **4g**, as most potent AChE inhibitors, was determined by a thioflavin-T fluorescent method [26,27]. Two aforementioned compounds were tested at 100 μM concentration and were compared with donepezil and rifampicin as reference drugs. The Aβ aggregation inhibition results were presented in Table 3. The selected compounds exhibited a promising inhibitory potency on self-induced $A\beta_{1\text{–}42}$ aggregation. The inhibition percentage of compound **4c** was 44.9%, being higher than that of donepezil and rifampicin (22.0% and 27.5% respectively, Table 3). The compound **4g** having 3-methyl group produced less reduction in thioflavin-T fluorescence (28.9%) than unsubstituted derivative **4c**. The selected compound exhibited less activity in AChE-induced $A\beta_{1\text{-}42}$ aggregation thioflavin-T assay than self-induced $A\beta_{1\text{-}42}$ aggregation.

2.5. Cytotoxicity against HepG2 cells

In order to evaluate the hepatotoxicity of the selected compounds (**4c** and **4g**), an in vitro cytotoxicity assay was conducted on HepG2 cell line. The percentage of the viable cells was determined at the different concentrations of compounds **4c** and **4g** (1–500 μM), in comparison with reference drug tacrine. As shown in Table 4, the percentage of the

Table 3
Inhibition of AChE-induced and self-induced $A\beta_{1\text{-}42}$ aggregation by compounds **4c** and **4g** using ThT assay.

Compound	Inhibition of Aβ aggregation (%)	
	Self-induced[a]	AChE-induced[b]
4c	44.9 ± 3.6	18.3 ± 8.5
4g	28.9 ± 1.5	12.1 ± 3.6
Donepezil	22.0 ± 5.4	26.1 ± 2.5
Rifampicin	27.5 ± 4.3	12.2 ± 3.0

[a] Inhibition of self-induced $A\beta_{1\text{-}42}$ aggregation (50 μM) produced by the tested compound at 100 μM concentration. Values are expressed as means ± SEM of three experiments.
[b] Co-aggregation inhibition of $A\beta_{1\text{-}42}$ and AChE by the tested compound at 100 μM concentration. Values are expressed as means ± SEM of three experiments.

Table 4
Viability (%) of HepG2 cells in the presence of **4c**, **4g**, and Tacrine.

Compound	Viability (%) HepG2 cells							
	1 μM	5 μM	10 μM	25 μM	50 μM	100 μM	300 μM	500 μM
4c	96.0 ± 1.5^{ns}	93.3 ± 1.6*	91.7 ± 1.7*	90.4 ± 2.2**	86.6 ± 2.3**	84.9 ± 2.3**	80.1 ± 1.7**	77.0 ± 2.4**
4g	98.2 ± 1.6^{ns}	97.4 ± 0.7^{ns}	95.1 ± 0.7^{ns}	92.8 ± 1.8*	89.8 ± 1.3*	86.5 ± 1.8**	82.2 ± 1.4**	80.0 ± 2.0**
Tacrine	92.5 ± 2.1*	88.3 ± 1.6**	81.4 ± 1.4**	76.4 ± 1.4**	63.4 ± 2.5**	54.5 ± 3.2**	47.3 ± 2.0**	35.9 ± 2.1**

Cell viability was evaluated by MTT assay. The obtained results from triplicate experiments were reported as mean ± SEM. The significant (**$p \leq 0.01$, *$p \leq 0.05$) or not significant (ns) values respect to control group were obtained after one-way ANOVA analysis followed by Newman-Keuls post hoc test.

viable cells was not remarkably changed in the presence of compounds **4c** and **4g** even at the concentration of 25 μM (viability > 90%), while tacrine decreased the cell viability to 76.4% at this concentration. Also, the effect of compounds **4c** and **4g** on cell viability was significantly lower than that of tacrine at high concentrations.

2.6. Neuroprotective activity of compounds 4c and 4g against H_2O_2-induced cell death in PC12 cells

The neuroprotective activity of the selected compounds **4c** and **4g** against H_2O_2-induced injury in differentiated PC12 cells was evaluated. As illustrated in Fig. 3, exposure of PC12 cells to H_2O_2 significantly reduced the cell viability to 30%, while pretreatment with various concentrations of both **4c** and **4g** (0.1–20 μM) significantly increased the viability in a dose-dependent manner.

2.7. Ligand-protein docking simulation

To understand the interaction mode of the tested compounds, **4c** as representative compound was selected and docked into the active site of acetylcholinesterase (1EVE). Considering the docking data analysis, the π-stacking and hydrophobic interactions are mainly responsible for the binding process. During the docking process the ligand was prone to locate at the vicinity of catalytic triad. The pendant benzyl moiety makes π-stacking with His439 and Trp83. The central pyridinium ring is attached to the Phe329 via π-cation interaction and π-stacking. Moreover, the positively charged nitrogen appeals to Asp71 through charge interaction. The schematic binding mode is depicted in Fig. 4 in 2D and 3D views.

2.8. Kinetics study of AChE inhibition

Kinetics study was done to figure out inhibition mechanism of compound **4c** as the best active compound toward the AChE. To obtain the Lineweaver-Burke graph, the enzyme activity was determined in the presence of four different concentrations of compared 4c as the best inhibitor (0, 7, 14, 28 nM) using different concentrations of substrate (ATChI, 0.14, 0.32, 0.70 μM). As depicted in Lineweaver-Burke graph (Fig. 5), the competitive inhibition could be realized (1/V is constant). This finding is in agreement with docking study in which the ligand particularly occupied the catalytic site. The double reciprocal plot was constructed to achieve inhibition constant. Hence the inhibition constant was 5.6 nM.

3. Conclusion

We have reported design, synthesis, molecular modeling and biological evaluation of a new series of benzylpyridinium salts bearing benzothiazole moiety. The target compounds were conveniently synthesized *via* the reaction between 2-aminothiophenol and pyridin-4-carbalehyde, followed by *N*-benzylation using various benzyl halides. The results of in vitro biological assay revealed that compounds **4c**, **4f**, **4g** and **4h** had potent anti-AChE activity comparable or more potent than standard drug donepezil at nanomolar levels (IC_{50} values = 14–23 nM). The anti-BuChE activity of all tested compounds was superior to standard drug donepezil (IC_{50} values = 0.18–2.20 μM), except for compounds **4m** and **4q**. Among the synthesized compounds, **4c** and **4g**, as potent AChE inhibitors were screened for their $A\beta_{1-42}$ anti-aggregating activity and neuroprotective property in PC12 cells. The biological results indicated that these compounds could remarkably inhibit self-induced $A\beta_{1-42}$ aggregation. Furthermore, the selected inhibitors could significantly protect PC12 cells against H_2O_2-induced damage. The kinetic study demonstrated that the prototype compound inhibits AChE in competitive manner. According to the ligand-enzyme docking simulation, compound **4c** occupied the active site at the vicinity of catalytic triad. These valuable results along with simple and affordable synthesis suggested that **4c** and **4g** can be used as new multi-targeted compounds toward development of effective disease-modifying drugs to treat AD.

4. Experimental

4.1. General chemistry

All reagents and materials were procured from Merck, Aldrich and Fluka chemical companies and used as received. Thin-layer chromatography (TLC) was done on silica gel 60 F_{254} plates (Merck). FT-IR spectra of products were recorded by a Bruker, Equinox 55 spectrometer. All melting points were measured by a Buchi melting point B-540B.V.CHI apparatus. A Bruker 500 MHz NMR instrument was used to record the ^{1}H NMR and ^{13}C NMR spectra using DMSO-d_6 as solvent. Mass spectra of the products were obtained with an Agilent technology (HP) 5973 Mass Selective Detector, operating at an ionization potential of 70 eV.

4.2. Synthesis of 2-(pyridin-4-yl)-1H-benzo[d]imidazole (3a)

A mixture of *o*-phenylenediamine (**1a**, 1 mmol), Fe_3O_4@NCs–OPO_3H (0.05 g) and absolute ethanol (2 mL) was put into a 25 mL round-bottom flask and stirred for 5 min at room temperature. Then, a solution of pyridin-4-carbalehyde (**2**, 1 mmol) in ethanol (2 mL) was added dropwise to this mixture at 50 °C under vigorous stirring for 2 h. After completion of reaction (monitored by TLC, *n*-hexane/EtOAc 70:30), the catalyst was isolated from reaction mixture by external magnet. Then, water and sodium carbonate were added to the reaction mixture and the separated solid was collected as pure product **3a**. Yield 92%; yellowish solid; mp 216–218 °C; IR (KBr, cm^{-1}) ν_{max}: 1610 (C=N). ^{1}H NMR (DMSO-d_6, 500 MHz) δ: 13.28 (s, 1H, NH), 8.76 (d, 2H, J = 5.5 Hz, H_a pyridine), 8.09 (d, 2H, J = 5.5 Hz, H_b pyridine), 7.73 (d, 1H, J = 7.8 Hz, H_4 benzimidazole), 7.59 (d, 1H, J = 7.8 Hz, H_7 benzimidazole), 7.30 (t, 1H, J = 7.8 Hz, H_5 benzimidazole), 7.24 (t, 1H, J = 7.8 Hz, H_6 benzimidazole). ^{13}C NMR (DMSO-d_6, 125 MHz) δ: 150.5, 148.8, 137.1, 124.5, 122.6, 120.3, 111.8. Anal. Calcd for $C_{12}H_9N_3$ (195.22): C, 73.83; H, 4.65; N, 21.52. Found: C, 73.72; H, 4.43; N, 21.74.

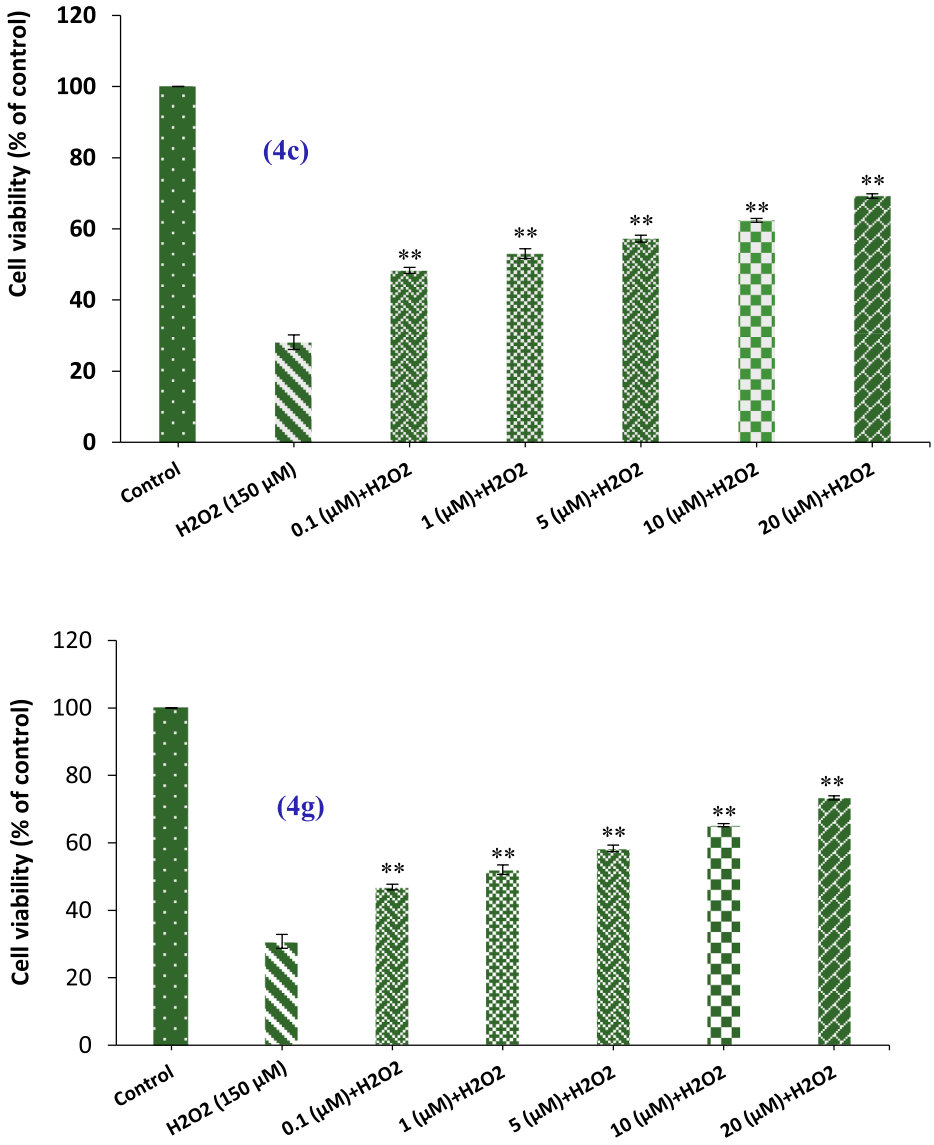

Fig. 3. Neuroprotective effect of compounds **4c** and **4g** against H_2O_2-induced cell death in PC12 cells. Each experiment was performed in triplicates and mean ± SEM of the obtained results were reported. The significant values ($p < 0.01$) compared to that of H_2O_2 group were represented by ** symbol.

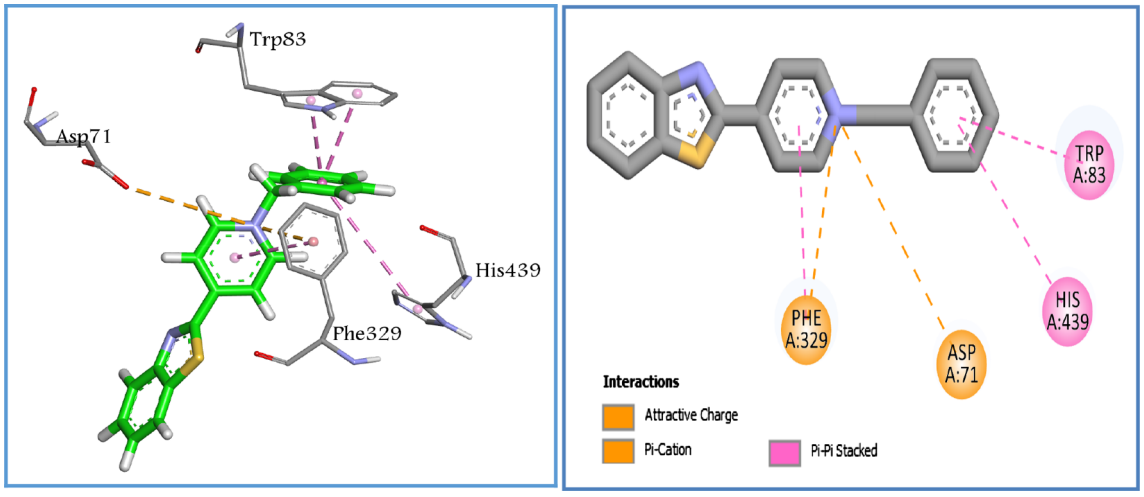

Fig. 4. The interaction of **4c** with the key residues in the active site of 1EVE.

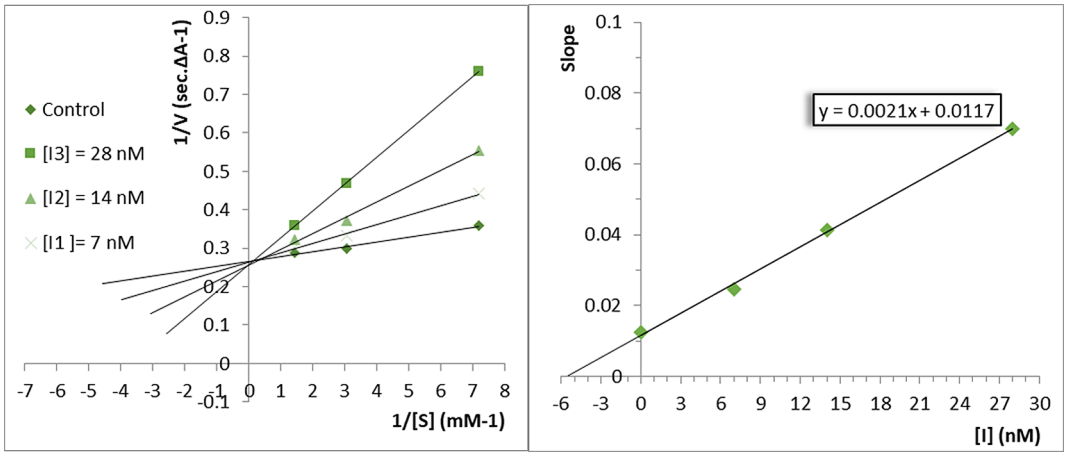

Fig. 5. *Left*: Lineweavere-Burk plot for the inhibition of AChE by compound **4c** at different concentrations of substrate (ATCh), *Right:* Secondary plot for calculation of steady state inhibition constant (K_i) of compound **4c**.

*4.3. Synthesis of 2-(pyridin-4-yl)benzo[d]oxazole (**3b**)*

In a mortar, a mixture of 2-aminophenol (**1b**, 1 mmol), pyridine-4-carbaldehyde (**2**, 1 mmol), $KMnO_4$ (3.4 mmol) and HOAc (0.08 mL) was ground at room temperature for 10 min. After completion of the reaction (as indicated by TLC, *n*-hexane/EtOAc 80:20), acetone (5 mL) was added to the reaction mixture and the mixture was filtered. After addition of water to the filtrated solution, the desired product **3b** was separated as a pure solid. Yield 81%; cream solid; mp 129–131 °C; IR (KBr, cm^{-1}) ν_{max}: 1614 (C=N). ^{1}H NMR (DMSO-d_6, 500 MHz) δ: 8.85 (d, 2H, J = 4.5 Hz, H_a pyridine), 8.11 (d, 2H, J = 4.5 Hz, H_b pyridine), 7.90 (d, 1H, J = 7.5 Hz, H_4 benzoxazole), 7.86 (d, 1H, J = 8.0 Hz, H_7 benzoxazole), 7.52 (t, 1H, J = 8.0 Hz, H_5 benzoxazole), 7.47 (t, 1H, J = 7.5 Hz, H_6 benzoxazole). ^{13}C NMR (DMSO-d_6, 125 MHz) δ: 160.3, 150.9, 150.4, 141.2, 133.5, 126.7, 125.4, 120.9, 120.5, 111.4. Anal. Calcd for $C_{12}H_8N_2O$ (196.20): C, 73.46; H, 4.11; N, 14.28. Found: C, 73.61; H, 4.34; N, 14.09.

*4.4. Synthesis of 2-(pyridin-4-yl)benzo[d]thiazole (**3c**)*

A mixture of 2-aminothiophenol (**1c**, 1 mmol), pyridine-4-carbaldehyde (**2**, 1 mmol) and Fe_3O_4@NCs–OPO_3H (0.05 g) was heated at 100 °C under solvent free condition for 90 min. The progress of the reaction was monitored by TLC (*n*-hexane/EtOAc 80:20). After completion of the reaction, the mixture was dissolved in hot ethanol and the catalyst was isolated by external magnet. The solid product was appeared by addition of water to the concentrated filtrate and then recrystallized from ethanol to give pure compound **3c**. Yield 94%; cream solid; mp 132–134 °C; IR (ATR, cm^{-1}) ν_{max}: 1594 (C=N). ^{1}H NMR (DMSO-d_6, 500 MHz) δ: 8.80 (d, 2H, J = 4.5 Hz, H_a pyridine), 8.23 (d, 1H, J = 8.0 Hz, H_4 benzothiazole), 8.15 (d, 1H, J = 8.0 Hz, H_7 benzothiazole), 8.03 (d, 2H, J = 4.5 Hz, H_b pyridine), 7.61 (t, 1H, J = 8.0 Hz, H_5 benzothiazole), 7.55 (t, 1H, J = 8.0 Hz, H_6 benzothiazole). ^{13}C NMR (DMSO-d_6, 125 MHz) δ: 165.0, 153.3, 151.0, 139.5, 134.8, 127.1, 126.4, 123.5, 122.7, 120.9. Anal. Calcd for $C_{12}H_8N_2S$ (212.27): C, 67.90; H, 3.80; N, 13.20. Found: C, 67.63; H, 3.71; N, 13.57.

*4.5. General procedure for the preparation of compounds **4a-q***

In a 25 mL round bottom flask, a mixture of compounds **3a**, **3b** or **3c** (1 mmol), benzyl halide derivative (1.2 mmol) and a catalytic amount of KI in dry acetonitrile (5 mL) was refluxed for 1–4 h. After completion of the reaction (as monitored by TLC, *n*-hexane/EtOAc 50:50), the reaction mixture was cooled and the solvent was removed under reduced pressure. Afterward, the residue was triturated with diethyl ether (5 mL) to obtain the pure products **4a-q**.

*4.5.1. 4-(1H-benzo[d]imidazol-2-yl)-1-benzylpyridinium bromide (**4a**) [28]*

Yellowish solid; mp 240–242 °C; IR (KBr, cm^{-1}) ν_{max}: 1638 (C=N^+), 1616 (C=N). ^{1}H NMR (DMSO-d_6, 500 MHz) δ: 13.88 (s, 1H, NH), 9.32 (d, 2H, J = 6.3 Hz, H_a pyridine), 8.75 (d, 2H, J = 6.3 Hz, H_b pyridine), 7.76 (bs, 2H, $H_{4,7}$ benzimidazole), 7.59 (d, 1H, J = 7.0 Hz, $H_{2,6}$ phenyl), 7.49–7.45 (m, 5H, phenyl), 7.38 (bs, 2H, $H_{5,6}$ benzimidazole), 5.88 (s, 2H, CH_2N^+). ^{13}C NMR (DMSO-d_6, 125 MHz) δ: 153.0, 146.3, 145.7, 145.4, 145.2, 144.4, 134.1, 129.3, 129.2, 129.1, 128.9, 125.3, 124.0, 117.9, 62.8. Anal. Calcd for $C_{19}H_{16}BrN_3$ (366.25): C, 62.31; H, 4.40; N, 11.47. Found: C, 62.49; H, 4.12; N, 11.30.

*4.5.2. 4-(benzo[d]oxazol-2-yl)-1-benzylpyridinium bromide (**4b**) [28]*

Cream solid; mp 238–240 °C; IR (KBr, cm^{-1}) ν_{max}: 1641 (C=N^+), 1612 (C=N). ^{1}H NMR (DMSO-d_6, 500 MHz) δ: 9.38 (d, 2H, J = 6.3 Hz, H_a pyridine), 8.80 (d, 2H, J = 6.3 Hz, H_b pyridine), 8.00 (d, 1H, J = 8.0 Hz, H_7 benzoxazole), 7.95 (d, 1H, J = 8.0 Hz, H_4 benzoxazole), 7.63 (t, 1H, J = 8.0 Hz, H_5 benzoxazole), 7.59 (d, 2H, J = 7.0 Hz, $H_{2,6}$ phenyl), 7.55 (t, 1H, J = 8.0 Hz, H_6 benzoxazole), 7.49–7.44 (m, 5H, phenyl), 5.95 (s, 2H, CH_2N^+). ^{13}C NMR (DMSO-d_6, 125 MHz) δ: 157.6, 150.9, 146.0, 141.2, 140.9, 134.1, 129.6, 129.3, 129.0, 128.3, 126.2, 125.3, 121.3, 111.8, 63.3. Anal. Calcd for $C_{19}H_{15}BrN_2O$ (367.24): C, 62.14; H, 4.12; N, 7.63. Found: C, 62.49; H, 4.18; N, 7.35.

*4.5.3. 4-(benzo[d]thiazol-2-yl)-1-benzylpyridinium bromide (**4c**) [28]*

Cream solid; mp 217–219 °C; IR (KBr, cm^{-1}) ν_{max}: 1635 (C=N^+), 1563 (C=N). ^{1}H NMR (DMSO-d_6, 500 MHz) δ: 9.34 (d, 2H, J = 6.5 Hz, H_a pyridine), 8.78 (d, 2H, J = 6.5 Hz, H_b pyridine), 8.35 (d, 1H, J = 7.8 Hz, H_7 benzothiazole), 8.26 (d, 1H, J = 8.5 Hz, H_4 benzothiazole), 7.70 (t, 1H, J = 8.5 Hz, H_5 benzothiazole), 7.65 (t, 1H, J = 8.0 Hz, H_6 benzothiazole), 7.59 (d, 2H, J = 6.5 Hz, $H_{2,6}$ phenyl), 7.50–7.47 (m, 3H, $H_{3,4,5}$ phenyl), 5.95 (s, 2H, $-CH_2N^+$). ^{13}C NMR (DMSO-d_6, 125 MHz) δ: 161.3, 153.3, 146.6, 145.8, 136.2, 134.2, 129.4, 129.3, 128.9, 127.9, 127.8, 125.3, 124.4, 123.2, 63.0. MS *m/z* (%) 303 (M^+, 0.4), 212 (1 0 0), 186 (13), 170 (5), 141 (3), 108 (13), 91 (92), 69 (12), 51 (7). Anal. Calcd for $C_{19}H_{15}BrN_2S$ (383.30): C, 59.54; H, 3.94; N, 7.31. Found: C, 59.78; H, 3.89; N, 7.19.

*4.5.4. 4-(benzo[d]thiazol-2-yl)-1-(2-methylbenzyl)pyridinium chloride (**4d**)*

Cream solid; mp 200–202 °C; IR (KBr, cm^{-1}) ν_{max}: 1630 (C=N^+), 1563 (C=N). ^{1}H NMR (DMSO-d_6, 500 MHz) δ: 9.15 (d, 2H, J = 6.0 Hz, H_a pyridine), 8.78 (d, 2H, J = 6.0 Hz, H_b pyridine), 8.35 (d, 1H, J = 7.5 Hz, H_7 benzothiazole), 8.26 (d, 1H, J = 7.5 Hz, H_4 benzothiazole), 7.69 (t, 1H, J = 7.5 Hz, H_5 benzothiazole), 7.65 (t, 1H,

J = 7.5 Hz, H_6 benzothiazole), 7.37–7.33 (m, 2H, $H_{4,6}$ phenyl), 7.30 (t, 1H, J = 7.5 Hz, H_5 phenyl), 7.25 (d, 1H, J = 7.5, H_3 phenyl), 5.99 (s, 2H, $-CH_2N^+$), 2.34 (s, 3H, CH_3). ^{13}C NMR (DMSO-d_6, 125 MHz) δ: 161.3, 153.3, 146.7, 146.0, 145.9, 137.1, 136.1, 132.0, 130.9, 129.7, 129.2, 127.8, 126.7, 125.3, 124.4, 123.2, 61.4, 18.8. MS *m/z* (%) 317 (M^+, 6), 212 (95), 186 (10), 143 (3), 127 (8), 105 (1 0 0), 77 (16), 51 (12). Anal. Calcd for $C_{20}H_{17}ClN_2S$ (352.88): C, 68.07; H, 4.86; N, 7.94. Found: C, 68.36; H, 4.81; N, 7.76.

4.5.5. 4-(Benzo[d]thiazol-2-yl)-1-(2-nitrobenzyl)pyridinium chloride ***(4e)***

Yellow solid; mp 228–229 °C; IR (KBr, cm^{-1}) ν_{max}: 1630 (C=N^+), 1564 (C=N). ^{1}H NMR (DMSO-d_6, 500 MHz) δ: 9.23 (d, 2H, J = 6.5 Hz, H_a pyridine), 8.85 (d, 2H, J = 6.5 Hz, H_b pyridine), 8.38 (d, 1H, J = 7.5 Hz, H_7 benzothiazole), 8.38 (d, 1H, J = 6.5 Hz, H_4 benzothiazole), 8.28 (d, 1H, J = 7.5 Hz, H_3 phenyl), 7.83 (t, 1H, J = 7.5 Hz, H_5 phenyl), 7.75 (t, 1H, J = 7.5 Hz, H_4 phenyl), 7.71 (t, 1H, J = 7.5 Hz, H_5 benzothiazole), 7.67 (t, 1H, J = 7.5 Hz, H_6 benzothiazol), 7.29 (d, 1H, J = 7.5 Hz, H_6 phenyl), 6.31 (s, 2H, $-CH_2N^+$). ^{13}C NMR (DMSO-d_6, 125 MHz) δ: 161.3, 153.4, 147.5, 147.0, 146.6, 146.5, 136.2, 134.9, 130.5, 129.2, 127.9, 125.6, 125.5, 125.3, 124.3, 123.3, 60.5. Anal. Calcd for $C_{19}H_{14}ClN_3O_2S$ (383.85): C, 59.45; H, 3.68; N, 10.95. Found: C, 59.66; H, 3.94; N, 10.61.

4.5.6. 4-(Benzo[d]thiazol-2-yl)-1-(2-chlorobenzyl)pyridinium chloride ***(4f)***

Yellow solid; mp 198–200 °C; IR (KBr, cm^{-1}) ν_{max}: 1628 (C=N^+), 1562 (C=N). ^{1}H NMR (DMSO-d_6, 500 MHz) δ: 9.23 (d, 2H, J = 6.5 Hz, H_a pyridine), 8.79 (d, 2H, J = 6.5 Hz, H_b pyridine), 8.36 (d, 1H, J = 8.0 Hz, H_7 benzothiazole), 8.26 (d, 1H, J = 7.5 Hz, H_4 benzothiazole), 7.69 (t, 1H, J = 7.5 Hz, H_5 benzothiazole), 7.66 (d, 1H, J = 7.5 Hz, H_3 phenyl), 7.62 (d, 1H, J = 8.5 Hz, H_6 phenyl), 7.55–7.47 (m, 3H, $H_{4,5}$ phenyl and H_6 benzothiazole), 6.08 (s, 2H, $-CH_2N^+$). ^{13}C NMR (DMSO-d_6, 125 MHz) δ: 161.2, 153.3, 146.9, 146.3, 146.1, 136.2, 133.2, 131.3, 130.1, 128.1, 127.8, 125.2, 125.1, 124.4, 124.3, 123.1, 61.0. MS *m/z* (%) 337 (M^+, 13), 301 (15), 212 (100), 186 (13), 125 (79), 89 (23), 63 (20). Anal. Calcd for $C_{19}H_{14}Cl_2N_2S$ (373.30): C, 61.13; H, 3.78; N, 7.50. Found: C, 61.39; H, 3.67; N, 7.36.

4.5.7. 4-(Benzo[d]thiazol-2-yl)-1-(3-methylbenzyl)pyridinium chloride ***(4g)***

Yellow solid; mp 190–192 °C; IR (KBr, cm^{-1}) ν_{max}: 1637 (C=N^+), 1564 (C=N). ^{1}H NMR (DMSO-d_6, 500 MHz) δ: 9.31 (d, 2H, J = 4.5 Hz, H_a pyridine), 8.75 (d, 2H, J = 4.5 Hz, H_b pyridine), 8.33 (d, 1H, J = 7.5 Hz, H_7 benzothiazole), 8.23 (d, 1H, J = 7.5 Hz, H_4 benzothiazole), 7.66 (d, 1H, J = 7.5 Hz, H_6 phenyl), 7.63 (d, 1H, J = 7.5 Hz, H_4 phenyl), 7.41–7.35 (m, 3H, H_5 phenyl and $H_{5,6}$ benzothiazole), 7.25 (d, 1H, J = 7.5 Hz, H_2 phenyl), 6.08 (s, 2H, $-CH_2N^+$), 2.32 (s, 3H, CH_3). ^{13}C NMR (DMSO-d_6, 125 MHz) δ: 161.2, 153.3, 146.5, 145.8, 145.6, 138.6, 136.1, 133.9, 130.0, 129.2, 127.8, 125.9, 125.3, 125.2, 124.4, 123.2, 63.0, 20.8. MS *m/z* (%) 317 (M^+, 6), 212 (91), 186 (8), 127 (7), 105 (1 0 0), 79 (13), 51 (10). Anal. Calcd for $C_{20}H_{17}ClN_2S$ (352.88): C, 68.07; H, 4.86; N, 7.94. Found: C, 68.29; H, 4.79; N, 7.71.

4.5.8. 4-(Benzo[d]thiazol-2-yl)-1-(3-fluorobenzyl)pyridinium chloride ***(4 h)***

Yellow solid; mp 200–202 °C; IR (KBr, cm^{-1}) ν_{max}: 1634 (C=N^+), 1588 (C=N). ^{1}H NMR (DMSO-d_6, 500 MHz) δ: 9.34 (d, 2H, J = 6.5 Hz, H_a pyridine), 8.78 (d, 2H, J = 6.5 Hz, H_b pyridine), 8.35 (d, 1H, J = 7.8 Hz, H_7 benzothiazole), 8.25 (d, 1H, J = 7.8 Hz, H_4 benzothiazole), 7.68 (t, 1H, J = 7.8 Hz, H_5 benzothiazole), 7.64 (t, 1H, J = 7.8 Hz, H_6 benzothiazole), 7.55–7.51 (m, 2H, $H_{5,6}$ phenyl), 7.45 (d, 1H, J = 7.5 Hz, H_2 phenyl), 7.30 (t, 1H, J = 8.5 Hz, H_4 phenyl), 5.96 (s, 2H, $-CH_2N^+$). ^{13}C NMR (DMSO-d_6, 125 MHz) δ: 162.2 (d, $^1J_{C\text{-}F}$ = 237.5 Hz), 161.2, 153.3, 146.7, 145.9, 145.8, 136.4, 136.2, 131.3, 127.8, 125.3 (d, $^3J_{C\text{-}F}$ = 12.5 Hz), 124.3 (d, $^2J_{C\text{-}F}$ = 18.7 Hz), 123.2 (d, $^3J_{C\text{-}F}$ = 12.5 Hz), 116.3, 116.0, 115.8 (d, $^2J_{C\text{-}F}$ = 18.7 Hz), 62.2. MS *m/z* (%) 321 (M^+, 2), 212 (85), 186 (12), 159 (4), 127 (4), 109 (1 0 0), 89 (14), 69 (16), 51 (8). Anal. Calcd for $C_{19}H_{14}ClFN_2S$ (356.84): C, 63.95; H, 3.95; N, 7.85. Found: C, 63.73; H, 3.76; N, 8.11.

4.5.9. 4-(Benzo[d]thiazol-2-yl)-1-(3-chlorobenzyl)pyridinium bromide ***(4i)***

Yellow solid; mp 216–219 °C; IR (KBr, cm^{-1}) ν_{max}: 1639 (C=N^+), 1565 (C=N). ^{1}H NMR (DMSO-d_6, 500 MHz) δ: 9.35 (d, 2H, J = 6.5 Hz, H_a pyridine), 8.78 (d, 2H, J = 6.5 Hz, H_b pyridine), 8.35 (d, 1H, J = 7.8 Hz, H_7 benzothiazole), 8.25 (d, 1H, J = 7.8 Hz, H_4 benzothiazole), 7.77 (s, 1H, H_2 phenyl), 7.69 (t, 1H, J = 7.8 Hz, H_5 benzothiazole), 7.64 (t, 1H, J = 7.8 Hz, H_6 benzothiazole), 7.58 (d, 1H, J = 6.0 Hz, H_6 phenyl), 7.53–7.50 (m, 2H, $H_{4,5}$ phenyl), 5.95 (s, 2H, $-CH_2N^+$). ^{13}C NMR (DMSO-d_6, 125 MHz) δ: 161.2, 153.3, 146.7, 145.9, 145.8, 136.2, 133.6, 131.0, 129.4, 128.9, 127.7, 125.4, 125.3, 124.4, 124.2, 123.1, 62.1. Anal. Calcd for $C_{19}H_{14}BrClN_2S$ (417.75): C, 54.63; H, 3.38; N, 6.71. Found: C, 54.94; H, 3.20; N, 6.55.

4.5.10. 4-(Benzo[d]thiazol-2-yl)-1-(3-bromobenzyl)pyridinium bromide ***(4j)***

Cream solid; mp 246–248 °C; IR (KBr, cm^{-1}) ν_{max}: 1635 (C=N^+), 1567 (C=N). ^{1}H NMR (DMSO-d_6, 500 MHz) δ: 9.37 (d, 2H, J = 6.0 Hz, H_a pyridine), 8.78 (d, 2H, J = 6.0 Hz, H_b pyridine), 8.35 (d, 1H, J = 7.8 Hz, H_7 benzothiazole), 8.25 (d, 1H, J = 7.8 Hz, H_4 benzothiazole), 7.91 (s, 1H, H_2 phenyl), 7.69–7.62 (m, 4H, H_5 benzothiazole and $H_{4,5,6}$ phenyl), 7.43 (t, 1H, J = 7.8 Hz, H_6 benzothiazole), 5.95 (s, 2H, $-CH_2N^+$). ^{13}C NMR (DMSO-d_6, 125 MHz) δ: 161.3, 153.3, 146.7, 145.9, 136.6, 136.2, 132.3, 131.8, 131.4, 128.1, 127.9, 127.8, 125.4, 124.4, 123.2, 122.3, 62.0. Anal. Calcd for $C_{19}H_{14}Br_2N_2S$ (462.20): C, 49.37; H, 3.05; N, 6.06. Found: C, 49.11; H, 3.13; N, 6.21.

4.5.11. 4-(Benzo[d]thiazol-2-yl)-1-(4-nitrobenzyl)pyridinium chloride ***(4k)***

Orange solid; mp 240–242 °C; IR (KBr, cm^{-1}) ν_{max}: 1635 (C=N^+), 1610 (C=N). ^{1}H NMR (DMSO-d_6, 500 MHz) δ: 9.40 (d, 2H, J = 6.0 Hz, H_a pyridine), 8.81 (d, 2H, J = 6.0 Hz, H_b pyridine), 8.01 (d, 1H, J = 7.8 Hz, H_7 benzothiazole), 7.95 (d, 1H, J = 7.8 Hz, H_4 benzothiazole), 7.64 (t, 1H, J = 7.8 Hz, H_5 benzothiazol), 7.61 (d, 1H, J = 7.0 Hz, $H_{3,5}$ phenyl), 7.56 (t, 1H, J = 7.8 Hz, H_6 benzothiazole), 7.49 (d, 1H, J = 7.0 Hz, $H_{2,6}$ phenyl), 5.97 (s, 2H, $-CH_2N^+$). ^{13}C NMR (DMSO-d_6, 125 MHz) δ: 157.6, 150.8, 146.0, 145.8, 141.1, 140.8, 134.0, 129.3, 129.1, 128.2, 126.2, 125.3, 121.3, 111.8, 63.3. Anal. Calcd for $C_{19}H_{14}ClN_3O_2S$ (383.85): C, 59.45; H, 3.68; N, 10.95. Found: C, 59.69; H, 3.55; N, 10.67.

4.5.12. 4-(Benzo[d]thiazol-2-yl)-1-(4-fluorobenzyl)pyridinium chloride ***(4l)***

Red solid; mp 242–243 °C; IR (KBr, cm^{-1}) ν_{max}: 1632 (C=N^+), 1601 (C=N). ^{1}H NMR (DMSO-d_6, 500 MHz) δ: 9.32 (d, 2H, J = 6.0 Hz, H_a pyridine), 8.78 (d, 2H, J = 6.0 Hz, H_b pyridine), 8.35 (d, 1H, J = 8.0 Hz, H_7 benzothiazole), 8.26 (d, 1H, J = 8.0 Hz, H_4 benzothiazole), 7.71–7.63 (m, 4H, $H_{5,6}$ benzothiazole and $H_{2,6}$ phenyl), 7.33 (t, 2H, J = 8.5 Hz, $H_{3,5}$ phenyl), 5.92 (s, 2H, $-CH_2N^+$). ^{13}C NMR (DMSO-d_6, 125 MHz) δ: 162.62 (d, $^1J_{C\text{-}F}$ = 245.0 Hz), 161.2, 153.3, 146.6, 145.8, 145.7, 136.2, 131.5, 130.3, 127.8, 125.3 (d, $^3J_{C\text{-}F}$ = 11.2 Hz), 124.35. 123.17, 116.1 (d, $^2J_{C\text{-}F}$ = 20.0 Hz), 62.24. MS *m/z* (%) 321 (M^+, 4), 212 (5), 127 (30), 109 (1 0 0), 93 (4), 83 (29), 69 (30), 61 (21), 51 (13). Anal. Calcd for $C_{19}H_{14}ClFN_2S$ (356.84): C, 63.95; H, 3.95; N, 7.85. Found: C, 63.61; H, 3.73; N, 8.08.

4.5.13. 4-(Benzo[d]thiazol-2-yl)-1-(4-bromobenzyl)pyridinium chloride ***(4m)***

Orange solid; mp 233–235 °C; IR (KBr, cm^{-1}) ν_{max}: 1631 (C=N^+), 1587 (C=N). ^{1}H NMR (DMSO-d_6, 500 MHz) δ: 9.31 (d, 2H, J = 5.5 Hz, H_a pyridine), 8.77 (d, 2H, J = 5.5 Hz, H_b pyridine), 8.35 (d, 1H, J = 7.5 Hz, H_7 benzothiazole), 8.25 (d, 1H, J = 7.5 Hz, H_4 benzothiazole), 7.69–7.64 (m, 4H, $H_{5,6}$ benzothiazole and $H_{3,5}$ phenyl), 7.57 (d, 2H, J = 7.5 Hz, $H_{2,6}$ phenyl), 5.92 (s, 2H, $-CH_2N^+$). ^{13}C NMR (DMSO-d_6, 125 MHz) δ: 161.2, 153.3, 146.6, 145.9, 145.7, 136.2, 133.3, 132.1, 131.2, 127.8, 125.4, 124.4, 124.2, 122.9, 62.2. Anal. Calcd for $C_{19}H_{14}BrClN_2S$ (417.75): C, 54.63; H, 3.38; N, 6.71. Found: C, 54.08; H, 3.16; N, 6.51.

4.5.14. 4-(Benzo[d]thiazol-2-yl)-1-(2-chloro-6-fluorobenzyl)pyridinium chloride (4n)

Yellow solid; mp 196–198 °C; IR (KBr, cm^{-1}) ν_{max}: 1632 (C=N^+), 1604 (C=N). ^{1}H NMR (DMSO-d_6, 500 MHz) δ: 9.17 (d, 2H, J = 6.2 Hz, H_a pyridine), 8.74 (d, 2H, J = 6.2 Hz, H_b pyridine), 8.35 (d, 1H, J = 7.8 Hz, H_7 benzothiazole), 8.26 (d, 1H, J = 8.5 Hz, H_4 benzothiazole), 7.69 (t, 1H, J = 7.5 Hz, H_5 phenyl), 7.66–7.62 (m, 2H, $H_{5,6}$ benzothiazole), 7.54 (d, 1H, J = 8.0 Hz, H_3 phenyl), 7.47 (t, 1H, J = 8.5 Hz, H_4 phenyl), 6.14 (s, 2H, $-CH_2N^+$). ^{13}C NMR (DMSO-d_6, 125 MHz) δ: 161.6 (d, $^1J_{C\text{-}F}$ = 250 Hz), 161.1, 153.4, 146.9, 146.1, 145.9, 136.2, 135.2, 133.4, 127.9, 126.4, 125.2 (d, $^3J_{C\text{-}F}$ = 11.2 Hz), 124.4 (d, $^2J_{C\text{-}F}$ = 17.5 Hz), 123.2 (d, $^3J_{C\text{-}F}$ = 10.0 Hz), 119.0 (d, $^2J_{C\text{-}F}$ = 16.2 Hz), 115.6, 55.0. MS m/z (%) 355 (M^+, 0.7), 186 (12), 212 (100), 143 (89), 107 (23), 69 (15), 45 (8). Anal. Calcd for $C_{19}H_{13}Cl_2FN_2S$ (391.29): C, 58.32; H, 3.35; N, 7.16. Found: C, 58.64; H, 3.20; N, 7.02.

4.5.15. 4-(Benzo[d]thiazol-2-yl)-1-(2,6-dichlorobenzyl)pyridinium chloride (4o)

Yellow solid; mp 213–214 °C; IR (KBr, cm^{-1}) ν_{max}: 1630 (C=N^+), 1577 (C=N). ^{1}H NMR (DMSO-d_6, 500 MHz) δ: 9.12 (d, 2H, J = 6.5 Hz, H_a pyridine), 8.73 (d, 2H, J = 6.5 Hz, H_b pyridine), 8.35 (d, 1H, J = 7.8 Hz, H_7 benzothiazole), 8.27 (d, 1H, J = 7.8 Hz, H_4 benzothiazole), 7.72–7.61 (m, 5H, $H_{5,6}$ benzothiazole and $H_{3,4,5}$ phenyl), 6.22 (s, 2H, $-CH_2N^+$). ^{13}C NMR (DMSO-d_6, 125 MHz) δ: 161.0, 153.4, 146.9, 145.8, 136.6, 136.3, 133.2, 129.6, 128.3, 127.9, 125.1, 124.5, 124.4, 123.2, 58.7. Anal. Calcd for $C_{19}H_{13}Cl_3N_2S$ (407.74): C, 55.97; H, 3.21; N, 6.87. Found: C, 55.62; H, 3.59; N, 6.99.

4.5.16. 4-(Benzo[d]thiazol-2-yl)-1-(2,4-dichlorobenzyl)pyridinium chloride (4p)

Yellowish solid; mp 216–218 °C; IR (KBr, cm^{-1}) ν_{max}: 1634 (C=N^+), 1589 (C=N). ^{1}H NMR (DMSO-d_6, 500 MHz) δ: 9.22 (d, 2H, J = 6.2 Hz, H_a pyridine), 8.79 (d, 2H, J = 6.2 Hz, H_b pyridine), 8.36 (d, 1H, J = 8.0 Hz, H_7 benzothiazole), 8.27 (d, 1H, J = 8.0 Hz, H_4 benzothiazole), 7.83 (s, 1H, H_3 phenyl), 7.70 (t, 1H, J = 8.0 Hz, H_5 benzothiazole), 7.66 (t, 1H, J = 8.0 Hz, H_6 benzothiazole), 7.59 (bs, 2H, $H_{5,6}$ phenyl), 6.05 (s, 2H, $-CH_2N^+$). ^{13}C NMR (DMSO-d_6, 125 MHz) δ: 161.2, 153.4, 147.0, 146.3, 146.2, 136.2, 135.3, 134.4, 132.8, 130.5, 129.7, 128.2, 127.9, 125.2, 124.5, 123.3, 60.4. Anal. Calcd for $C_{19}H_{13}Cl_3N_2S$ (407.74): C, 55.97; H, 3.21; N, 6.87. Found: C, 55.60; H, 3.40; N, 7.08.

4.5.17. 4-(Benzo[d]thiazol-2-yl)-1-(3,4-dichlorobenzyl)pyridinium chloride (4q)

Orange solid; mp 227–229 °C; IR (KBr, cm^{-1}) ν_{max}: 1632 (C=N^+), 1562 (C=N). ^{1}H NMR (DMSO-d_6, 500 MHz) δ: 9.31 (d, 2H, J = 6.3 Hz, H_a pyridine), 8.78 (d, 2H, J = 6.3 Hz, H_b pyridine), 8.35 (d, 1H, J = 8.0 Hz, H_7 benzothiazole), 8.26 (d, 1H, J = 8.0 Hz, H_4 benzothiazole), 7.97 (s, 1H, H_2 phenyl), 7.76 (d, 1H, J = 7.8 Hz, H_5 phenyl), 7.70 (t, 1H, J = 8.0 Hz, H_5 benzothiazole), 7.66 (t, 1H, J = 7.8 Hz, H_6 benzothiazole), 7.61 (d, 1H, J = 8.5 Hz, H_6 phenyl), 5.91 (s, 2H, $-CH_2N^+$). ^{13}C NMR (DMSO-d_6, 125 MHz) δ: 161.2, 153.3, 146.8, 146.0, 145.1, 136.2, 134.7, 132.3, 131.7, 131.3, 129.5, 127.9, 125.4, 125.3, 124.6, 123.2, 61.6. Anal. Calcd for $C_{19}H_{13}Cl_3N_2S$ (407.74): C, 55.97; H, 3.21; N, 6.87. Found: C, 55.66; H, 3.56; N, 6.95.

4.6. In vitro AChE/BuChE inhibition assay

The inhibition potential of the synthesized compounds toward AChE (*Electrophorus electricus)* and BuChE (equine serum) was assessed using spectrophotometric method of Ellman [29]. Donepezil was selected as reference drug. Five different concentrations of each compound were tested to obtain 20–80% enzyme inhibition. The test medium, consisted of 2 mL phosphate buffer (0.1 M, pH 8.0), 60 μL of 5,5′-dithio-bis(2-nitrobenzoic acid) (DTNB, 0.01 M), each enzyme separately (20 μL of 2.5 unit/mL) and 30 μL of compound solution was incubated at 25 °C for 5 min and then, 20 μL of substrate (acetylthiocholine iodide or butyrylthiocholine iodide) was added. As a reference, a solution containing all ingredients except the synthesized compounds was used. Changes in absorbance were measured at 412 nm for 2 min at 25 °C and inhibition percent of compounds was determined. The IC_{50} values were obtained by the method of plotting log concentration *vs.* percentage of inhibition.

4.7. Determination of the inhibitory potency on self-induced and AChE-induced $A\beta_{1\text{-}42}$ aggregation

Inhibition of self-induced and AChE-induced aggregation of amyloid β protein 1–42 was determined using a thioflavin-T (ThT)-based fluorescence assay [27]. $A\beta_{1\text{-}42}$ protein (Sigma A9810) was dissolved in phosphate buffer saline pH 7.4 (PBS, HyClone Thermo Scientific) containing 1% ammonium hydroxide at a concentration of 50 μM and incubated for 72 h at 37 °C for prefibrillation. Afterwards, $A\beta_{1\text{-}42}$ (10 μL) ± human recombinant AChE (0.01 u/mL, Sigma C1682) were added to 0.05 M KP buffer (pH = 7.4) and incubated at 37 °C for 48 h in the absence and presence of inhibitors (100 μM). Incubated mixture (100 μL) was mixed with 50 μL of thioflavin-T (ThT, 200 μM) in 50 mM glycine-NaOH buffer (pH 8.5) and decrease in the ThT fluorescence intensity at 448 nm (λ_{exc} (and 490 nm (λ_{em}) was measured using a SpectraMax® Microplate Reader at 48 h. Rifampicin (100 μM, Sigma R-3501) and Donepezil (100 μM, Sigma D-6821) were also tested as reference compounds. Self or AChE-induced aggregation percents due to the presence of the tested compounds were determined by the following calculation: $[(IF_i/IF_o) \times 100]$ where IF_i and IF_o are the fluorescence intensities obtained for Aβ ± AChE in the presence and in the absence of inhibitors.

4.8. Cytotoxicity assay of the selected compounds on HepG2 cell line

Cytotoxicity of the selected compounds (**4c** and **4g**) against HepG2 cell line (human hepatocellular carcinoma) was determined using MTT-based assay. After culturing of the cell line (purchased from Iranian biological resource center, IBRC, Tehran, Iran) in DMEM medium fortified by FBS (10%) at 37 °C under 5% CO_2, the cells were harvested and seeded (15000 cells/well) in 96 well microplate wells and allowed to attach for 24 h at the same conditions. Thereafter, desired concentration (1–500 μM) of each compound (dissolved in FBS-free DMEM medium) was added to the related well and the microplate was incubated for further 24 h. In the next step, the medium of each well was replaced by MTT solution (5 mg/mL) and incubated for 4 h until the formazan crystal was formed which was then dissolved by addition of DMSO (100 μL). The related absorbance (540 nm) was consequently measured using a Synergy 2 multi-mode plate reader apparatus (Biotek, Winooski, VT, USA) and applied to determine the viability percent regarding to that of the control. All above mentioned experiments were performed in triplicate and mean of the obtained results was reported.

4.9. Neuroprotection assay against H_2O_2-induced cell death in PC12 cells

In order to determine the neuroprotective effect of the selected compounds **4c** and **4g** against H_2O_2-induced cell death in PC12 cells (neuron-like rat derived adrenal pheochromocytoma cell line), the cell line (provided by Iranian biological resource center, Tehran, Iran) was cultivated in Dulbecco's minimal essential medium supplemented by FBS (10%), penicillin (100 U/mL), and streptomycin (100 μg/mL) at 37 °C and 5% CO_2 in a humidified incubator. The cells were harvested at logaritmic phase and seeded (10,000 cells per well) into 96-well tissue culture microplate and allowed to adhere to well bottom for 24 h. Thereafter, desired concentration of compounds **4c** and **4g** (0.1–20 μM) were added to the related well before being exposed by H_2O_2 (final concentratin of 150 μM) for 6 h. The culture medium of each well was

then replaced by DMEM medium containing MTT (5 mg/mL) and incubated for 4 h. Consequently, the precipitated formazan crystals were dissolved by 100 μL DMSO followed by recording the related absorbance at 570 nm using a Synergy2 multi-mode microplate reader (BioTek, USA) and calculating the viabilty percent compared to that of the control group. All experminets were carried out in triplicates and mean of the obtained results were reported [30].

4.10. Docking simulations

Docking studies were performed using the Molecular Operating Environment (MOE) software (Chemical Computing Group, Montreal, Canada). The crystal structure of acetylcholinesterase complexed with donepezil (1EVE) was retrieved from the Protein Data Bank (PDB). The preparation and optimization of the receptor were done by Autodock Tools (4.2) [31]. The ligand 3D structure and minimization prepared by Openbabel (2.3.1). The dimensions of active site box were set as 15 × 15 × 15 Å, the center of grid box was placed at x = 2.023, y = 63.295, z = 67.062. The 3D molecular visualization of the strongest cluster was done by Discovery Studio 2.0 software.

Acknowledgments

This work was supported financially by a grant from The Institute of Pharmaceutical Sciences (TIPS), Tehran University of Medical Sciences (grant number: 38526) and Iran National Science Foundation (INSF, grant number: 94003365).

References

[1] 2016 Alzheimer's disease facts and figures, Alzheimers Dement 12 (2016) 459–509.
[2] S.F. Razavi, M. Khoobi, H. Nadri, A. Sakhteman, A. Moradi, S. Emami, A. Foroumadi, A. Shafiee, Synthesis and evaluation of 4-substituted coumarins as novel acetylcholinesterase inhibitors, Eur. J. Med. Chem. 64 (2013) 252–259.
[3] S. Hamulakova, P. Poprac, K. Jomova, V. Brezova, P. Lauro, L. Drostinova, D. Jun, V. Sepsova, M. Hrabinova, O. Soukup, P. Kristian, Z. Gazova, Z. Bednarikova, K. Kuca, M. Valko, Targeting copper(II)-induced oxidative stress and the acetylcholinesterase system in Alzheimer's disease using multifunctional tacrine-coumarin hybrid molecules, J. Inorg. Biochem. 161 (2016) 52–62.
[4] J.L. Sussman, M. Harel, F. Frolow, C. Oefner, A. Goldman, L. Toker, I. Silman, Atomic structure of acetyicholinesterase from Torpedo cal fornica: A prototypicn acetyicholine-binding protein, Science 253 (1991) 872–879.
[5] E. Giacobini, Cholinesterases: New roles in brain function and in Alzheimer's disease, Neurochem. Res. 28 (2003) 515–522.
[6] L.-L. Shen, G.-X. Liu, Y. Tang, Molecular docking and 3D-QSAR studies of 2-substituted 1-indanone derivatives as acetylcholinesterase inhibitors, Acta Pharmacol. Sin. 28 (2007) 2053–2063.
[7] C. Zou, E. Montagna, Y. Shi, F. Peters, L. Blazquez-Llorca, S. Shi, S. Filser, M.M. Dorostkar, J. Herms, Intraneuronal APP and extracellular Abeta independently cause dendritic spine pathology in transgenic mouse models of Alzheimer's disease, Acta Neuropathol. 129 (2015) 909–920.
[8] Q. Shen, Q. Peng, J. Shao, X. Liu, Z. Huang, X. Pu, L. Ma, Y.M. Li, A.S. Chan, L. Gu, Synthesis and biological evaluation of functionalized coumarins as acetylcholinesterase inhibitors, Eur. J. Med. Chem. 40 (2005) 1307–1315.
[9] P. Gonzalez-Naranjo, N. Perez-Macias, N.E. Campillo, C. Perez, V.J. Aran, R. Giron, E. Sanchez-Robles, M.I. Martin, M. Gomez-Canas, M. Garcia-Arencibia, J. Fernandez-Ruiz, J.A. Paez, Cannabinoid agonists showing BuChE inhibition as potential therapeutic agents for Alzheimer's disease, Eur. J. Med. Chem. 73 (2014) 56–72.
[10] W.W. Chen, X. Zhang, W.J. Huang, Role of physical exercise in Alzheimer's disease, Biomed. Rep. 4 (2016) 403–407.
[11] P. Anand, B. Singh, A review on cholinesterase inhibitors for Alzheimer's disease, Arch. Pharm. Res. 36 (2013) 375–399.
[12] S. Ghanei-Nasab, M. Khoobi, F. Hadizadeh, A. Marjani, A. Moradi, H. Nadri, S. Emami, A. Foroumadi, A. Shafiee, Synthesis and anticholinesterase activity of coumarin-3-carboxamides bearing tryptamine moiety, Eur. J. Med. Chem. 121 (2016) 40–46.
[13] M. Khoobi, M. Alipour, A. Sakhteman, H. Nadri, A. Moradi, M. Ghandi, S. Emami, A. Foroumadi, A. Shafiee, Design, synthesis, biological evaluation and docking study of 5-oxo-4,5-dihydropyrano[3,2-c]chromene derivatives as acetylcholinesterase and butyrylcholinesterase inhibitors, Eur. J. Med. Chem. 68 (2013) 260–269.
[14] M.Y. Wu, G. Esteban, S. Brogi, M. Shionoya, L. Wang, G. Campiani, M. Unzeta, T. Inokuchi, S. Butini, J. Marco-Contelles, Donepezil-like multifunctional agents: Design, synthesis, molecular modeling and biological evaluation, Eur. J. Med. Chem. 121 (2016) 864–879.
[15] P. Costanzo, L. Cariati, D. Desiderio, R. Sgammato, A. Lamberti, R. Arcone, R. Salerno, M. Nardi, M. Masullo, M. Oliverio, Design, synthesis, and evaluation of donepezil-like compounds as AChE and BACE-1 Inhibitors, ACS Med. Chem. Lett. 7 (2016) 470–475.
[16] F. Abedinifar, S.M.F. Farnia, M. Mahdavi, H. Nadri, A. Moradi, J.B. Ghasemi, T.T. Kucukkilinc, L. Firoozpour, A. Foroumadi, Synthesis and cholinesterase inhibitory activity of new 2-benzofuran carboxamide-benzylpyridinum salts, Bioorg. Chem. 80 (2018) 180–188.
[17] F. Baharloo, M.H. Moslemin, H. Nadri, A. Asadipour, M. Mahdavi, S. Emami, L. Firoozpour, R. Mohebat, A. Shafiee, A. Foroumadi, Benzofuran-derived benzylpyridinium bromides as potent acetylcholinesterase inhibitors, Eur. J. Med. Chem. 93 (2015) 196–201.
[18] J.S. Lan, Y. Ding, Y. Liu, P. Kang, J.W. Hou, X.Y. Zhang, S.S. Xie, T. Zhang, Design, synthesis and biological evaluation of novel coumarin-N-benzyl pyridinium hybrids as multi-target agents for the treatment of Alzheimer's disease, Eur. J. Med. Chem. 139 (2017) 48–59.
[19] H. Akrami, B.F. Mirjalili, M. Khoobi, H. Nadri, A. Moradi, A. Sakhteman, S. Emami, A. Foroumadi, A. Shafiee, Indolinone-based acetylcholinesterase inhibitors: synthesis, biological activity and molecular modeling, Eur. J. Med. Chem. 84 (2014) 375–381.
[20] M. Alipour, M. Khoobi, A. Foroumadi, H. Nadri, A. Moradi, A. Sakhteman, M. Ghandi, A. Shafiee, Novel coumarin derivatives bearing N-benzyl pyridinium moiety: potent and dual binding site acetylcholinesterase inhibitors, Bioorg. Med. Chem. 20 (2012) 7214–7222.
[21] W.E. Klunk, Y. Wang, G.-F. Huang, M.L. Debnath, D.P. Holt, L. Shao, R.L. Hamilton, M.D. Ikonomovic, S.T. DeKosky, C.A. Mathis, The binding of 2-(4'-methylaminophenyl)benzothiazole to postmortem brain homogenates is dominated by the amyloid component, J. Neurosci. 23 (2003) 2086–2092.
[22] L. Huang, T. Su, W. Shan, Z. Luo, Y. Sun, F. He, X. Li, Inhibition of cholinesterase activity and amyloid aggregation by berberine-phenyl-benzoheterocyclic and tacrine-phenyl-benzoheterocyclic hybrids, Bioorg. Med. Chem. 20 (2012) 3038–3048.
[23] L. Jiang, M. Zhang, L. Tang, Q. Weng, Y. Shen, Y. Hu, R. Sheng, Identification of 2-subsituted benzothiazole derivatives as triple-functional agents with potential for AD therapy, RSC Adv. 6 (2016) 17318–17327.
[24] I. Diner, J. Dooyema, M. Gearing, L.C. Walker, N.T. Seyfried, Generation of clickable Pittsburgh compound B for the detection and capture of β-amyloid in Alzheimer's disease brain, Bioconjug. Chem. 28 (2017) 2627–2637.
[25] B.F. Mirjalili, A. Bamoniri, E. Bagheri, $KMnO_4$/HOAc system promoted one-pot synthesis of benzoxazoles from *o*-aminophenols or oxidative cyclization of *o*-hydroxyarylidene anilines at room temperature, J. Iran. Chem. Soc. 13 (2015) 809–814.
[26] P. Camps, X. Formosa, C. Galdeano, T. Gómez, D. Muñoz-Torrero, M. Scarpellini, E. Viayna, A. Badia, M.V. Clos, A. Camins, M. Pallàs, M. Bartolini, F. Mancini, V. Andrisano, J. Estelrich, M. Lizondo, A. Bidon-Chanal, F.J. Luque, Novel donepezil-based inhibitors of acetyl- and butyrylcholinesterase and acetylcholinesterase-induced β-amyloid aggregation, J. Med. Chem. 51 (2008) 3588–3598.
[27] H. Levine, Thioflavine T interaction with synthetic Alzheimer's disease β-amyloid peptides: Detection of amyloid aggregation in solution, Protein Sci. 20 (1993) 404–410.
[28] P.P. Zarin, É.S. Lavrinovich, A.K. Aren, Pyridinium salts I. Reduction of 4-(benzazol-2-yl)pyridinium salts in a neutral medium, Chem. Heterocyclic Compd. 10 (1974) 92–95.
[29] G.L. Ellman, K.D. Courtney, V. Andres, R.M. Featherstone, A new and rapid colorimetric determination of acetyl cholinesterase activity, Biochem. Pharmacol. 7 (1961) 88–95.
[30] Z. Datki, A. Juhász, M. Gálfi, K. Soós, R. Papp, D. Zádori, B. Penke, Method for measuring neurotoxicity of aggregating polypeptides with the MTT assay on differentiated neuroblastoma cells, Brain Res. Bull. 62 (2003) 223–229.
[31] G.M. Morris, R. Huey, W. Lindstrom, M.F. Sanner, R.K. Belew, D.S. Goodsell, A.J. Olson, AutoDock4 and AutoDockTools4: Automated docking with selective receptor flexibility, J. Comput. Chem. 30 (2009) 2785–2791.